Control of pool boiling incipience in confined space: dynamic morphing of the wall effect

Laetitia LEAL[1], Pascal LAVIEILLE [1], Marc MISCEVIC [1*], François PIGACHE [1], Lounès TADRIST [2]

* Corresponding author: Tel.: ++33 (0)5 61 55 83 07; Fax: ++33 (0)5 61 55 60 21; Email:
marc.miscevic@laplace.univ-tlse.fr
[1]LAboratoire PLAsma et Conversion de l'Energie, France
[2] Laboratoire IUSTI, France

Abstract A new active heat transfer enhancement and control technique is proposed in this work. One of the major aims of the technique is to decrease pool boiling incipience temperature by dynamic morphing imposed to confinement wall. Dynamic deformation generates variation of pressure which increases the fluid metastability level. An experimental device was built to evaluate boiling incipience temperature. Experimental results were compared with hydrodynamic and nucleation models.

Keywords: Multiphase Flow, Micro Flow, Pool Boiling, Heat Transfer Enhancement, Active Technique, Wall Morphing, Cavitation Phenomena

1. Introduction

Cooling needs are constantly growing both in the high-tech industry and in conventional fields. Numerous works have been performed to enhance heat transfer and numerous improvements proposed (Webb, 1994, for example, has identified 13 of them). These techniques can be classified in two types: passive and active. Passive techniques consist in increasing heat transfer without input of external power. This can be achieved by increasing the exchange surface area and/or by disrupting boundary layers and/or by changing fluid properties. Currently, it is passive techniques of heat transfer enhancement that are mainly used. However, in many configurations, the need to increase heat and mass transfer further involves the input of additional energy to achieve this goal and is becoming more frequently considered. Various solutions have been explored. The most frequently studied are electro-hydrodynamic (EHD) techniques (Laohalertdecha, 2007), jets (Jambunata, 2009) and spray cooling (Kim, 2007), and the use of sonic and ultrasonic vibrations (Kim, 2004). Combining passive and active techniques to reach high compactness is another challenge. In this way, the use of phase change processes in micro-

geometries is one of the most promising solutions (Agostini, 2007). To achieve this, certain obstacles must be overcome. Among them, one major problem in thermal management systems involving boiling is the high temperatures that must be reached to obtain the onset of boiling. One way to avoid this problem is to increase the liquid metastability level by temporarily decreasing the pressure of the liquid. In confined space, dynamic deformation of the surface with low absolute amplitude (but high relative amplitude) may lead to significant changes of the liquid pressure in the channel. So, dynamic morphing imposed on the confinement wall potentially appears as an interesting solution to control the onset of nucleation and thus to obtain boiling incipience at a lower wall temperature.

The purpose of the present work is to study the effects of the confinement wall dynamic deformation on pool boiling incipience in a narrow horizontal space. The effect of the deformation frequency is determined experimentally. Simplified models were generated to evaluate pool-boiling incipience versus dynamic deformation parameters. Experimental and theoretical results are discussed and compared.

2. Experimental set-up and procedure

2.1 Experimental set-up
An experimental device was designed and built to study pool-boiling incipience induced by dynamic deformation of the confinement wall. A schematic diagram of the experimental device is shown in figure 1.
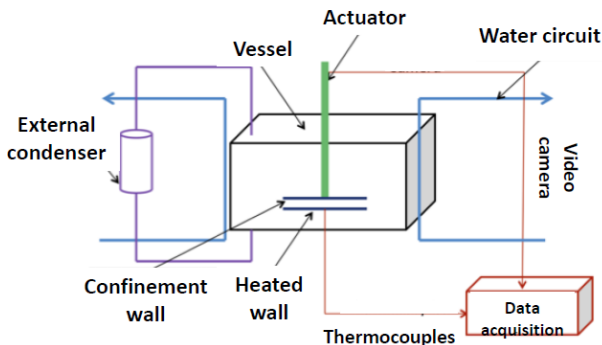

Figure 1: Experimental device scheme

Experiments were performed using n-pentane at atmospheric pressure (T_{sat}=309K). The pressure was maintained constant during all the experiments. The working fluid was maintained at 308.5K thanks to thermostated water flowing inside the vessel walls.

The test section placed inside the vessel is composed of a heated wall and a confinement wall. The heated wall was a 56 mm diameter aluminum cylinder block isolated on its bottom by 4 cm of Teflon ($\lambda = 0.25\text{W.m}^{-1}.\text{K}^{-1}$). A 40 mm diameter electrical resistance was placed 4 mm beneath the top surface of the aluminum cylinder to provide an imposed heat flux. Ten thermocouples located 2 mm beneath the heated surface were used to determine the wall temperature at different locations of the heating surface. The free surface of the liquid pool in the vessel was held at nearly 30 mm above the heated surface.

The top surface of the aluminum cylinder was polished in order to obtain a mean ruggedness around 0.1 μm. A 58 mm diameter confinement wall was placed above and parallel to the heating surface. The confinement wall was a 4 mm thick stainless steel plate. The distance between the top of the aluminum cylinder and the confinement plate

was adjustable from 50μm to 1mm with an accuracy of 30μm. It was dynamically deformed at its center whereas its periphery was maintained fixed. Significant wall morphing was obtained by using a piezoelectric actuator. The deformation amplitude range was from 0 to 250 μm and the deformation frequency range from 0 to 300Hz. Figure 2 reports schematically the deformation cycle of the confinement wall. A microscope objective with a low field depth fixed on a displacement stage controlled by a micrometer was placed parallel to the stainless steel wall axis. The profile of the static deformation of the confinement wall was then determined with an accuracy of 15μm. This system was also used to evaluate dynamic deformation. Figure 3 reported static deformation of confinement wall: a constant force was applied on the center of confinement plate. Only part of the confinement plate was deformed. Maximum dynamic deformation was assumed to have a similar shape to static deformation. The range of frequencies was chosen to avoid the resonant mode of wall confinement.
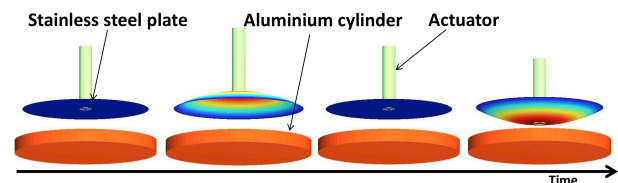

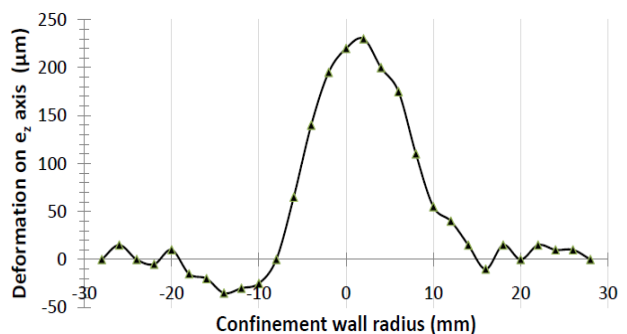**Figure 2: Confinement wall deformation**

Figure 3: Example of deformation profile obtained when a constant force is applied in the center of the stainless steel plate.

The main parameters imposed in the experiments were the thickness of the space between the aluminum cylinder and the confinement plate, and the amplitude and

frequency of the deformation.

2.2 Experimental procedure

Before each series of experiments, n-pentane was degassed to extract incondensable gases. The fluid was maintained at 310K for one hour. Simultaneously, intense boiling was imposed at the heated plate for 20 minutes to degas its surface. A condenser open to the atmosphere was placed at the top of the vessel so that the n-pentane condensed while the non-condensable gases were evacuated. This operation was repeated twice.

During the experiments, the fluid temperature was maintained slightly below the saturation temperature (at 308.5K) to reduce the occurrence of boiling phenomena other than on the heated surface. The heat flux was increased step by step (figure 4). Steady state was reached nearly 12 minutes after the increase of the heat flux was applied. The pool boiling incipience was detected by the appearance of a decrease of the wall temperature. So, maximum wall temperature prior to the onset of boiling defined the boiling incipience temperature.
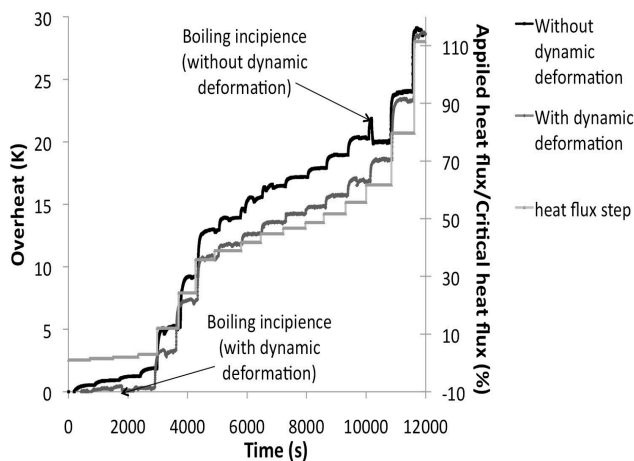

Figure 4: Effect of heat flux level on overheat without dynamic deformation (e=625μm, a₀=0μm, f=0Hz) and with dynamic deformation (e=625μm, a₀=210μm, f=100Hz)

Figure 4 reports wall superheating in response to a step of heat flux, with and without dynamic deformation. Wall superheat is defined as the difference between maximum wall temperature and saturation temperature at atmospheric pressure:

$$\Delta T_{w,max} = T_{w,max} - T_{sat}(p_{atm})$$

As the heat losses through the sides of the aluminum cylinder were significant, the spatial distribution of the heat flux is unknown. For these reasons, the ordinate in figure 4 was described by the ratio between the applied heat flux and the critical heat flux. The critical heat flux was evaluated thanks to the work of Stutz (Stutz (2009)) at $8W/cm^2$ at the confined configuration without dynamic deformation. Figure 4 highlights the deformation effect on pool boiling incipience temperature. Without dynamic deformation, pool boiling incipience superheating is about 22K whereas with dynamic deformation (f=100Hz, a₀=210μm, e=625μm) boiling incipience superheating is dramatically reduced to about 0.2K.

This example shows the significant effect of confinement wall dynamic deformation on pool boiling incipience wall superheating. A systematic analysis was performed to determine the effects of the frequency of the deformation on pool boiling incipience.

3. Experimental results

The parameters of the experiments carried out to determine the frequency effect on boiling incipience were slightly different from those considered in fig. 4:

- the distance between the top surface of the aluminum cylinder and the confinement plate (e) was 580μm (instead of 625 μm in fig. 4);
- the maximum amplitude of the deformation (a₀) was 210μm;
- the range of frequency was 0 (i.e., without actuator) to 100Hz.

Each experiment was carried out three times to check reproducibility.

Figure 5 reports the frequency effect on pool boiling incipience wall superheating. Diamonds indicate boiling incipience overheating obtained experimentally for each of the working conditions. Squares are the average of the three boiling incipience superheating values obtained for each frequency.

The maximum of scattering around the mean value is 3.1K, showing a relatively good reproducibility of the results. Experiments

highlight a nearly linear decrease of boiling incipience overheating when the frequency is increased. Many mechanisms may explain such a decrease. One is related to the liquid pressure variation that may change saturation conditions considerably. The increase of the dynamic deformation frequency brings about an increase of liquid pressure oscillation over time. During the time when liquid pressure is reduced, overheating of the liquid is temporarily increased due to a decrease of the saturation temperature. The rise of liquid overheating may be large enough to reach the conditions necessary for the onset of boiling. Then, both boiling and cavitation phenomena have to be considered.

For a better understanding of the effect of dynamic deformation on boiling incipience wall superheating, a hydrodynamic model and a nucleation model were designed. These models are described in section 4.
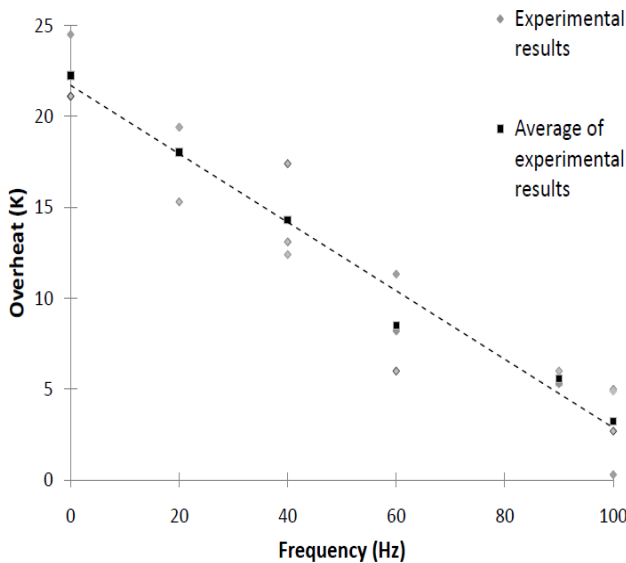

Figure 5: Effect of frequency on pool boiling incipience wall overheating (e=580µm, a$_0$=210µm)

4. Theoretical results

4.1 Hydrodynamic model

The aim of the hydrodynamic model is to evaluate the pressure oscillation of the liquid when dynamic deformation of the confinement wall is imposed. More particularly, the model must predict the minimum instantaneous value of the liquid pressure.

Figure 6 shows the geometric parameters considered. The scale is not respected in this scheme for clarity reasons. The diameter (D) of the confinement plate is much larger than the confinement distance (e). Ω is the volume of fluid contained between the aluminum cylinder and the confinement plate.
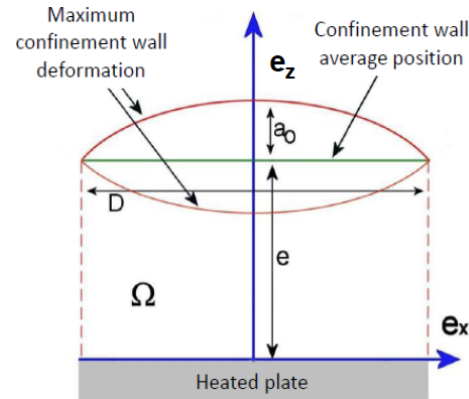

Figure 6: Geometric definitions

During experiments, fluid is highly confined (aspect ratio e/D is about 10^{-3}). The maximum amplitude of the deformation (a$_0$) has the same order of magnitude as the confinement distance (e). So, the radius of curvature $R = \frac{a}{2} + \frac{D^2}{8a} \approx \frac{D^2}{8a}$ is high.

As the aspect ratio e/D is high, when the actuator is in operation, streamlines are not very distorted. The problem may thus be assumed to be one-dimensional. Evaluation of the order of magnitude of the different terms in the momentum balance shows that the viscous stresses can be ignored compared to inertia. So, the main assumptions of the model are that flow is radial, the liquid is non-viscous and incompressible, and the physical properties are constant. Furthermore, the deformation of the membrane is assumed to be sinusoidal over time:

$$a(t) = a_o sin(\omega t)$$

Figure 7 represents a cross-section in the plane (**e$_x$**, **e$_y$**) of the volume Ω used to define the integration domain and the boundary limits (as well as their numbering). Ω is defined as $\Omega(t) = \{M(r, \theta, z)/r \in [0, x], \theta \in [-\theta_1, \theta_1], z \in [0, Z(x, t)]\}$. S$_1$ is the flow section at position r. S$_2$ and S$_2$' are the lateral surfaces of Ω. S$_3$ is the
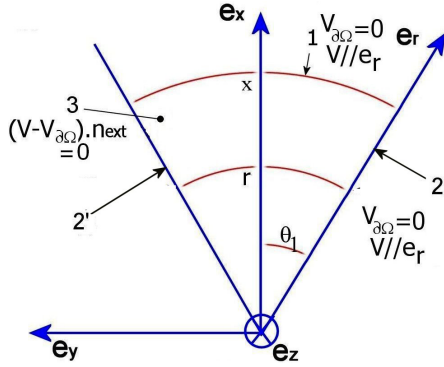
confinement plate surface.

Figure 7: Boundaries definition

The mass and momentum equations are written for the domain Ω:

$$\frac{\partial}{\partial t}\int_{\Omega}\rho d\Omega + \int_{\partial\Omega}\rho(\boldsymbol{V}-\boldsymbol{V_{\partial\Omega}})\boldsymbol{n}dS = 0 \qquad (1)$$

$$\frac{\partial}{\partial t}\int_{\Omega}\rho\boldsymbol{V}d\Omega + \int_{\partial\Omega}\rho\boldsymbol{V}(\boldsymbol{V}-\boldsymbol{V_{\partial\Omega}}).\boldsymbol{n}dS$$

$$= -\oint_{\partial\Omega}p\boldsymbol{n}dS \qquad (2)$$

Using equation 1 and assuming that the liquid is incompressible, velocity is expressed as:

$$\bar{V}(x,t) = -\frac{a_0\omega cos(\omega t)(\frac{x}{2}-\frac{x^3}{D^2})}{a(t)+e-4a(t)\frac{x^2}{D^2}} \qquad (3)$$

Equation 2 is projected onto $\boldsymbol{e_x}$ axis:

$$-\oint_{\partial\Omega}p(r,z(r,t))\boldsymbol{n}.\boldsymbol{e_x}dS =$$

$$2sin\theta_1[-x\bar{p}(x,t)Z(x,t)+$$

$$\int_0^x \bar{p}(r,t)Z(r,t)dr$$

$$+\int_0^x rp(r,Z(r,t))\frac{\partial Z(r,t)}{\partial r}dr] \qquad (4)$$

Assuming that $p(x,Z(x,t)) = K(x)\bar{p}(x,t)$, the last term of equation 4 becomes:

$$2sin\theta_1\int_0^x rp(r,Z(r,t))\frac{\partial Z(r,t)}{\partial r}dr$$

$$\cdot = 2sin\theta_1\int_0^x rK(r)\bar{p}(r,t)\frac{\partial Z(r,t)}{\partial r}dr \qquad (5)$$

$K(x)$ is a parameter representing the three dimensional effects. Assuming the pressure is homogenous along the z axis (due to the high confinement) leads to $K(x)=1$.

The mean value of the square of the velocity appears in the left term of equation (2). We assumed that it is related to the square of the mean velocity by:

$$\bar{V}^2(x,t) = \xi\bar{V}^2(x,t) \qquad (6)$$

Sensitivity analysis validated that ξ has very little influence on the minimum instantaneous pressure. Using the ideal fluid hypothesis, the parameter ξ is assumed to be equal to 1.

Finally, the dynamic deformation effect on pressure can be described by the following differential equation:

$$xZ(x,t)\frac{\partial\bar{p}(x,t)}{\partial x} - x\bar{p}(x,t)\frac{\partial Z(x,t)}{\partial x}(1-K(x))$$

$$= -\rho x(\bar{V}(x,t)\frac{\partial Z(x,t)}{\partial t}+Z(x,t)\frac{\partial\bar{V}(x,t)}{\partial t})$$

$$-\rho\xi\bar{V}(x,t)(\bar{V}(x,t)Z(x,t)+2xZ(x,t)\frac{\partial\bar{V}(x,t)}{\partial x}$$

$$+x\bar{V}(x,t)\frac{\partial Z(x,t)}{\partial x}) \qquad (7)$$

This hydrodynamic model allows the evaluation of the effects of frequency and amplitude of the deformation, as well as the confinement distance on pressure oscillations. Figure 9 reports minimum liquid pressure as a function of frequency, considering a confinement distance of 580µm and an amplitude of deformation of 210µm.

The minimum pressure of the liquid decreases continuously as the frequency increases. In the range of frequencies considered in this paper, the maximum value of the depression (for f=100Hz) is about 130 hPa. This value appears to be non-negligible; it corresponds to a decrease of the saturation temperature of approximately 4.3K. The effect of the reduction of the liquid pressure through the dynamic deformation of the confinement plate may thus play an important role in boiling incipience. To determine if this effect can explain the experimental results, the nucleation process has to be modeled. A simple approach

is detailed in the next section to evaluate the overheating needed to start the boiling process.
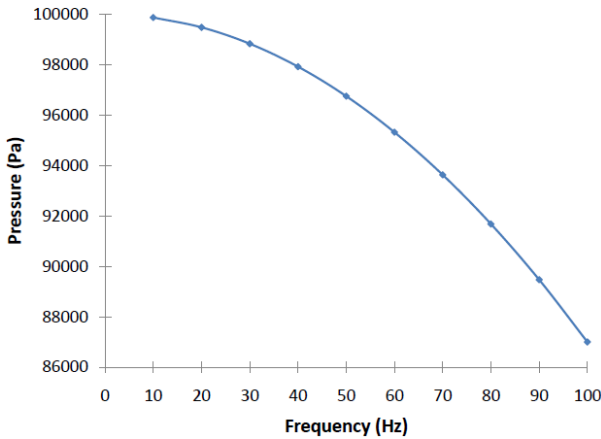

Figure 8: Minimum pressure versus frequency (e=580μm, a$_0$=210 μm)

4.2 Nucleation model

The nucleation model presented here allows us to evaluate the temperature of a bubble at equilibrium radius r$_c$ when the liquid pressure is imposed (Carey, 1992). It is assumed that when the equilibrium temperature is reached, a fluctuation of temperature (or pressure) implies the onset of boiling.

One major hypothesis is that vapor embryos are trapped in wall cavities prior to boiling incipience. Indeed, as the mean roughness of the top surface of the aluminum cylinder is about 0.1 μm, n-pentane vapor may be trapped in nucleation sites.

Assuming that the equilibrium radius of the embryos can be estimated by wall cavity characteristic dimensions, and using the Laplace equation, pool boiling incipience overheating is evaluated using the following equation:

$$\frac{p_l - p_{sat}(T_l)}{\rho_l} = \frac{p_v}{\rho_v} ln(\frac{p_v}{p_{sat}(T_l)}) \qquad (8)$$

T$_l$ is determined by imposing p$_l$ and using Clapeyron's equation to link p$_{sat}$ and T$_l$, while p$_v$ is related to p$_l$ by the Laplace equation (taking into account the variations of the latent heat of vaporization and of the surface tension with the temperature).

Figure 9 reports the liquid pressure as a function of wall superheating, according to equation (8). Experimental boiling incipience overheating without a confinement wall is consistent with the models choosing r$_c$=0.2μm (ΔT$_{ONB,exp}$=24.3K, ΔT$_{ONB,th}$=24.6K).
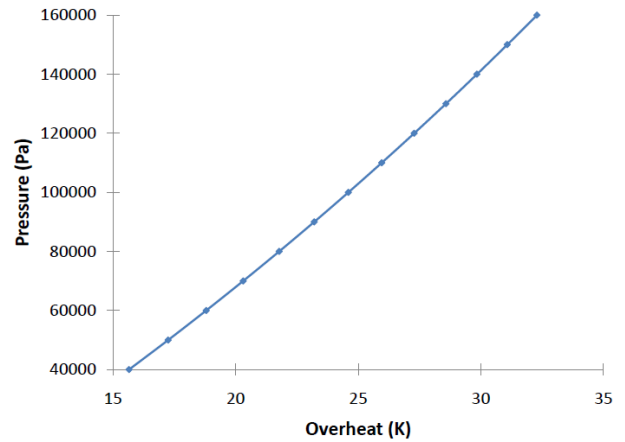

Figure 9: Variation of the liquid pressure as a function of wall superheating according to the nucleation model (r$_c$=0.2μm)

The order of magnitude of the cavity radius is the same of mean roughness (~ 0.1 μm). As expected, wall superheating decreases when the liquid pressure decreases. Nevertheless, the variations are small. For a pressure decrease of 130 hPa, the decrease of wall superheating is only about 2K while the saturation temperature decreases by 4.3K, as previously indicated. The difference in the decrease of wall superheating compared to the saturation temperature may be attributed to the change in the slope of the n-pentane saturation curve. For T~309K (wall superheating ~0K), this slope is dp/dT~3200Pa.K^{-1} while for T~333K (wall superheating ~24K) it is dp/dT~5400Pa.K^{-1}. Adding the effect of surface tension variation due to the temperature change, wall superheating decrease falls to 2K.

To summarize, the hydrodynamic model allows us to calculate the maximum decrease in the liquid pressure when dynamic deformation is considered (as a function of confinement distance, frequency and amplitude of the deformation).

Wall superheating at boiling incipience can be evaluated, in a first approach, by considerations of equilibrium thermodynamics. Merging these two models, boiling incipience can be correlated to the parameters of the dynamic deformation.

5. Comparison of theoretical and experimental results

Table 1 reports the pool boiling incipience temperatures without dynamic deformation. It compares boiling incipience temperatures when the fluid is confined (e=580μm) and when it is not confined (e>50mm). Experimental and theoretical results are compared. In this case, pressure is maintained constant (p=p_{sat}=1bar). Regarding the nucleation model, pool boiling incipience is assumed to be independent of confinement level. Table 1 reports the nucleation model and experimental results: theoretical results are consistent with experimental results. Nevertheless, an increase is observed in boiling onset temperature in the confined situation. This result are already been reported in previous works (Dupont (2003)).

e	$\Delta T_{ONB,th}$ (K)	$\Delta T_{max,ONB,exp}$ (K)
580μm	24.6	22.3
50mm		24.3

Table 1: Comparison of theoretical and experimental pool boiling incipience temperatures without dynamic deformation

Experimental and theoretical results are reported in figure 10. For both curves, boiling incipience temperature decreases linearly as deformation frequency increases. Table 2 indicates the pool boiling incipience temperatures obtained theoretically and experimentally. With dynamic deformation, large discrepancies were obtained between experimental and theoretical results. In the range of frequencies considered, the decrease in wall superheating was about 2K according to the nucleation model while it was about 20K experimentally. These differences stress that incipience temperature decrease is not only due to pressure reduction. Other mechanisms have to be taken into account in the theoretical model to explain such a large difference in wall superheating. One can speculate on the effect of transient phenomena, convection, etc. Further studies need to be conducted to clarify this point.

f (Hz)	$p_{min, th}$ (Pa)	$\Delta T_{ONB,th}$ (K)	$\Delta T_{max,ONB,exp}$ (K)
20	99480	24.4	18.0
40	97920	24.2	14.3
60	95319	23.8	8.5
70	93629	23.6	4.7
80	91679	23.3	12.9
90	89469	23.0	5.6
100	86998	22.6	3.2

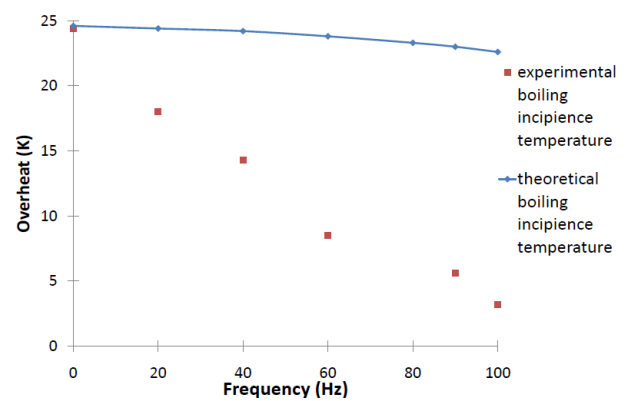**Table 2: Comparison between theoretical and experimental boiling incipience temperatures (e=580μm, a_0=210μm)**

Figure 10: Comparison between theoretical and experimental boiling incipience temperatures (e=580μm, a_0=210μm)

Conclusion

A new active heat transfer enhancement and control technique is presented in this work. It consists in dynamically deforming a confinement wall.

The experimental device used and the results obtained with it are presented. Pool boiling incipience temperatures were significantly reduced by dynamic deformation. For a deformation amplitude of 210μm and confinement distance of 625μm, wall superheating at boiling incipience nearly disappeared when the frequency reached 100Hz.

Analysis of the effect of frequency on boiling incipience superheating indicated that a frequency rise decreases the temperature of boiling incipience. The experimental results were compared with results of a hydrodynamic model coupled with a nucleation model. When the actuator was powered-off, pool boiling

incipience temperatures obtained experimentally were consistent with standard nucleation modeling. However, when the actuator was powered-on, theoretical and experimental results were significantly different. This indicates that incipience temperature decrease is not only due to pressure reduction.

Nomenclature

a	amplitude	m
a_0	maximum amplitude	m
∂_Ω	boundary	
D	confinement surface diameter	m
e	confinement distance	m
$\mathbf{e_x}, \mathbf{e_y}, \mathbf{e_z}$	unit vector of fixed reference frame	
$\mathbf{e_r}$	unit vector of rotating reference frame	
f	frequency	Hz
K	$p(x, Z(x,t)) = K(x)\bar{p}(x,t)$	
$\mathbf{n}$	normal vector	
p	pressure	Pa
$\bar{p}$	averaged pressure along $\mathbf{e_z}$	Pa
r	radial coordinate	m
r_c	equilibrium embryo radius	m
R	radius of curvature	m
S	surface area	m^2
t	time	s
T	temperature	K
V	speed	$m.s^{-1}$
$\bar{V}$	averaged speed along $\mathbf{e_z}$	$m.s^{-1}$
x	abscissa	m
z	ordinate	m
Z	confinement plate height	m

Greek symbols

θ_1	Angle between ($\mathbf{e_r}$, $\mathbf{e_x}$)	rad
ξ	$\overline{V^2}(x,t) = \xi \bar{V}^2(x,t)$	
λ	conductivity	$W.m^{-1}K^{-1}$
ρ	fluid volume mass	$kg.m^{-3}$
γ	surface tension	$N.m^{-1}$
ω	pulse	s^{-1}
Ω	volume	m^3

Subscripts

exp	experimental
l	liquid
max	maximum
min	minimum
ONB	onset of boiling
sat	saturation
th	theoretical
v	vapour
w	wall

Acknowledgment

References

Agostini B., Fabbri M., Park J. E., Wojtan L., Thome J. R., Michel B., 2007, State of the art of high heat flux cooling technologies, Heat Transfer Engineering, 28(4), 258-281

Carey V. P., 1992, Liquid-Vapour Phase Change Phenomena, Taylor & Francis, Philadelphia, 127-167

Dupont V., Miscevic M., Joly J.L., Platel V., 2003, Boiling incipience of highly wetting liquids in horizontal confined space, International Journal of Heat and Mass Transfer, 46, 4245-4256

Jambunathan K., Lai E., Moss M., Button B., 2009, A review of heat-transfer data for circular jet impingement, International Journal of Heat and Fluid Flow, 13 (2), 106-115

Kim H., Kim Y., Kang B., 2004, Enhancement of natural convection and pool boiling heat transfer via ultrasonic vibration, International Journal of Heat And Mass Transfer, 47 (12-13), 2831–2840.

Kim J., 2007, Spray cooling heat transfer: the state of the art, International Journal of Heat and Fluid Flow, 28 (4, Sp. Iss. SI), 753–767

Laohalertdecha S., Naphon P., Wongwises S., 2007, A review of electrohydrodynamic enhancement of heat transfer, Renewable and Sustainable Energy Reviews 11, 858-876

Stutz B., Lallemand M., Raimbault F., Passos J., 2009, Nucleate and transition boiling in narrow horizontal spaces, Heat and Mass Transfer, 45(7), 929-935

R. Webb, 1994, Principles of Enhanced Heat Transfer, Wiley Inter- science.